iScience

CellPress
OPEN ACCESS

Article

Genetic and functional analysis reveals *TENM4* contributes to schizophrenia

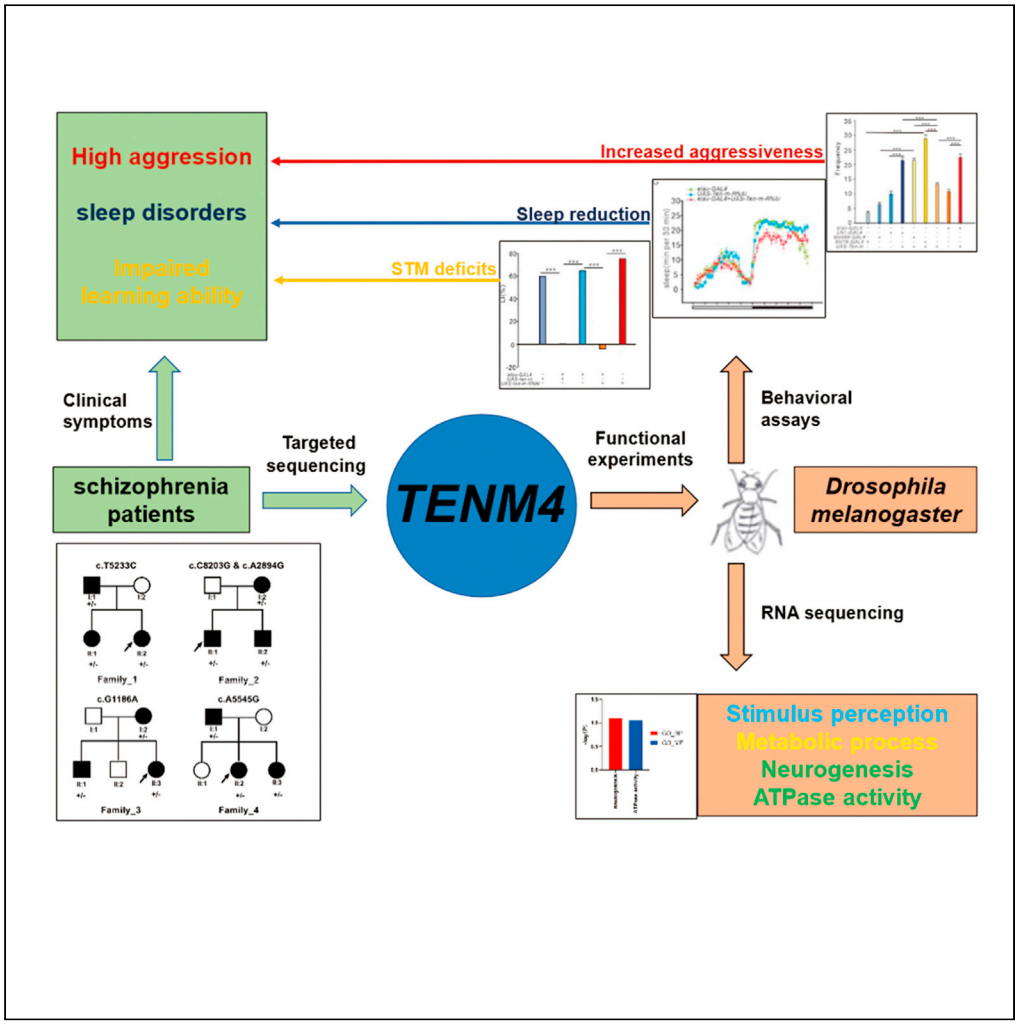

Xin Yi, Minzhe Li, Guang He, ..., Lin He, Yong Ping, Daizhan Zhou

helin@bio-x.cn (L.H.)
yoping@sjtu.edu.cn (Y.P.)
zhoudaizhan@sjtu.edu.cn (D.Z.)

Highlights

Possible pathogenic rare missense mutations in *TENM4* gene contribute to SCZ

Aberrant expression of *Ten-m* leads to behavioral disturbances related to SCZ symptoms

Ten-m affects stimulation, metabolic process, neurogenesis, and ATPase activity

Yi et al., iScience *24*, 103063
September 24, 2021
https://doi.org/10.1016/j.isci.2021.103063

iScience

CellPress
OPEN ACCESS

Article

Genetic and functional analysis reveals *TENM4* contributes to schizophrenia

Xin Yi,[1,4] Minzhe Li,[1,4] Guang He,[1,2,4] Huihui Du,[1] Xingwang Li,[1,2] Dongmei Cao,[1] Lu Wang,[1] Xi Wu,[1] Fengping Yang,[1] Xu Chen,[3] Lin He,[1,2,*] Yong Ping,[1,2,*] and Daizhan Zhou[1,5,*]

SUMMARY

***TENM4*, encoding a member of the teneurin protein family, is a risk gene shared by many types of mental diseases and is implicated in neuronal plasticity and signaling. However, the role and the mechanisms of *TENM4* in schizophrenia (SCZ) remain unclear. We identified possible pathogenic mutations in the *TENM4* gene through target sequencing of *TENM4* in 68 SCZ families. We further demonstrated that aberrant expression of *Ten-m* leads to lower learning ability, sleep reduction, and increased aggressiveness in animal models. RNA sequencing showed that aberrant expression of *Ten-m* was related to stimulus perception and metabolic process, and Gene Ontology enrichment terms were neurogenesis and ATPase activity. This study provides strong evidence that *TENM4* contributes to SCZ, and its functional mutations might be responsible for the impaired neural circuits and behaviors observed in SCZ.**

INTRODUCTION

Schizophrenia (SCZ) is a severe psychiatric disorder with high heritability, genetic heterogeneity, and polygenic effect (Kavanagh et al., 2015). It has been reported that SCZ shares the same risk genes and pathways as common mental diseases, including bipolar disorder, autism, depression, Alzheimer disease, mental retardation, and epilepsy (Sullivan et al., 2012). Previous studies have confirmed that *TENM4* is associated with bipolar disorder (Psychiatric GWAS Consortium Bipolar Disorder Working Group, 2011) (Ikeda et al., 2018) (Ivorra et al., 2014) (Heinrich et al., 2013), autism (Iossifov et al., 2014), and essential tremor (Hor et al., 2015) (Yan et al., 2020) (Chao et al., 2016). In most genome-wide association studies (GWAS) of SCZ, the common single-nucleotide polymorphisms (SNPs) in *TENM4* did not reach genome-wide significance. However, a case-control replication study showed that an SNP (rs12290811) located in *TENM4* was associated with SCZ (Ivorra et al., 2014). A whole-exome sequencing study in an SCZ family also identified one missense mutation co-segregated with the SCZ in *TENM4* (Xue et al., 2018). A genome-wide meta-analysis with individuals of East Asian or European ancestry identified 176 loci associated with SCZ, including *TENM4* (Lam et al., 2019). These studies partly provided some genetic evidence for *TENM4* as an important candidate gene for SCZ.

TENM4, also known as ODZ4, is a member of the teneurin protein family, which comprises large transmembrane proteins (Baumgartner et al., 1994). The *TENM4* gene is highly conserved among species (Tucker and Chiquet-Ehrismann, 2006). The temporal and spatial expression of teneurin family proteins in *Drosophila* (Baumgartner et al., 1994), zebrafish (Feng et al., 2002), birds (Tucker et al., 2000), and mice (Zhou et al., 2003) showed that Tenm4 protein was highly expressed in the nervous system, particularly in the brain. In *Drosophila*, a study showed that Ten-m acts as a synaptic cooperative matching molecule between the axons of olfactory receptor neurons (ORNs) and the dendrites of projecting neurons (PNs) in the olfactory system, and Ten-m could also guide synapses to achieve specific matches by homophilic interactions to ensure proper matching between neurons, indicating Ten-m plays an important role in neuron orientation (Hong et al., 2012). In addition, Ten-m was required for the organization and target selection of synapses in neurons (Mosca et al., 2012). In mice, a mutation in *Tenm4* suppressed oligodendrocyte differentiation and myelination of small-diameter axons (Suzuki et al., 2012). Knockdown expression of *Tenm4* in Neuro-2a cell lines decreased the length of individual neurites, while overexpression of *Tenm4* promoted cellular protrusion formation and neurite outgrowth (Suzuki et al., 2014). These studies indicated that aberrant expression of *Ten-m* might lead to mis-matched neural circuits.

[1]Bio-X Institutes, Key Laboratory for the Genetics of Developmental and Neuropsychiatric Disorders (Ministry of Education), Shanghai Jiao Tong University, 1954 Huashan Rd., Shanghai 200030, PR China

[2]Shanghai Key Laboratory of Psychotic Disorders, Shanghai Mental Health Center, Shanghai Jiao Tong University School of Medicine, Shanghai, China

[3]Department of Neurology, Shanghai Eighth People's Hospital, Shanghai Sixth People's Hospital Xuhui Branch, School of Medicine, Shanghai Jiao Tong University, Shanghai, PR China

[4]These authors contribute equally

[5]Lead contact

*Correspondence: helin@bio-x.cn (L.H.), yoping@sjtu.edu.cn (Y.P.), zhoudaizhan@sjtu.edu.cn (D.Z.)

https://doi.org/10.1016/j.isci.2021.103063

Table 1. Genetic analysis of *TENM4* in SCZ

FAM_ID	Position	Allele	SNP	AA_Change	AF	No.	Interpro_domain
Family_1	78,399,126	A > G	Ns	p.S1745P	ns	7	YD repeats
Family_2	78,369,210	G > C	rs527857070	p.Q2735E	1.605×10^{-5}	6	Tox-GHH domain
	78,443,605	T > C	rs141471364	p.N965S	0.0053	3	Carboxypeptidase-like, regulatory domain
Family_3	78,574,076	C > T	rs3812723	p.V396I	0.0003	3	.
Family_4	78,383,326	T > C	rs772977333	p.T1849A	0.0002	9	YD repeats

SNP, single-nucleotide polymorphism; AA, amino acid; AF, allele frequency; No. the number of software that supported the damaging effect of the missense mutation on TENM4 protein function.

Based on these previously reported findings, we hypothesized that *TENM4* plays an important role in SCZ development and contributes to SCZ-related clinical symptoms, such as learning disability, sleep disorders, and violent behavior. Patients with SCZ often show violence, social withdrawal, learning and memory declines, and sleep disorders (Dowd and Barch, 2012; Cohrs, 2008; Patel et al., 2014). To verify this hypothesis, we performed targeted sequencing of *TENM4* in 68 SCZ families to investigate the genetic contribution of *TENM4* on SCZ. Then, to identify the role of *TENM4* in SCZ, we examined the phenotypic characteristics by knockdown and overexpression of *Ten-m* in *Drosophila* and evaluated the effects of *Ten-m* on learning ability, sleep behavior, and aggressive behaviors. We also used mRNA sequencing to reveal the potential affected signaling pathways and molecular mechanisms of *TENM4*.

RESULTS

Rare missense mutations in *TENM4* are co-segregated with disease status in SCZ families

To determine whether rare mutations in *TENM4* are the candidate causal variants of SCZ, we initially performed whole *TENM4* exome sequencing in 351 subjects from 68 SCZ families. A total of 36 mutations in *TENM4* were identified using a step-by-step depth, quality filtering method. Then, 17 noncoding and synonymous variants were filtered to remove, and 19 nonsynonymous variants were kept. The 19 variants were annotated by ANNOVAR software (2019Oct24) with dbnsfp35c, gnomad211_exome, avsnp150, and intervar_20,180,118 databases to evaluate the function and allele frequency in the population. Given the pattern of dominant inheritance in the families, only rare heterozygous variants (allele frequency<1%) shared by the patients but not found in the normal controls in the same family were considered to be candidate mutations. At last, we found 5 variants were co-segregated with SCZ in their families, which were p.S1745P in Family_1, p.Q2735E and p.N965S in Family_2, p.V396I in Family_3, and p.T1849A in Family_4 (Table 1 and Figure 1A). In addition, all the five missense mutations were predicted to be deleterious to the *TENM4* protein function by no less than three software.

Meanwhile, to confirm the relationship between *TENM4* and SCZ, we re-analyzed the data from the genome-wide association analysis in a total of 50,874 SCZ cases and 83,493 controls from the Chinese and PGC2 genome-wide meta-analysis (Li et al., 2017). We analyzed 1196 SNPs in the region (chr11: 78,358,876-79,156,992) and found that 39 SNPs showed nominally significant association with SCZ ($p < 0.01$, Figure 1B).

Ten-m affects the learning abilities in *Drosophila*

To investigate the potential contribution of *TENM4* to SCZ, we examined the function of *Ten-m* in the *Drosophila* nervous system. We used the courtship conditioning assay, a behavioral assay that tests the courtship short-term memory (STM) to indicate learning ability (Siegel and Hall, 1979). After selection at the eclosion stage, male flies that had never mated were solely paired with mated females whose cuticles had already obtained cis-vaccenyl acetate (cVA), a male-specific and volatile pheromone, from males on mating (Everaerts et al., 2010). The males would be rejected by the mated females; then, the males formed STM, resulting in the suppression of courtship behavior when placed with other mated female flies over a period of time (Siwicki et al., 2005). The reduction of suppression indicates a lack of STM and the damage to learning ability. We used courtship indices (CIs), calculated as the percentage of courtship duration within 10 min, and learning indices (LIs), generated by the relative difference between the mean CIs of naive and trained male flies, to quantify the STM. Our data revealed that males of control genotypes (*elav-GAL4*, *UAS-*

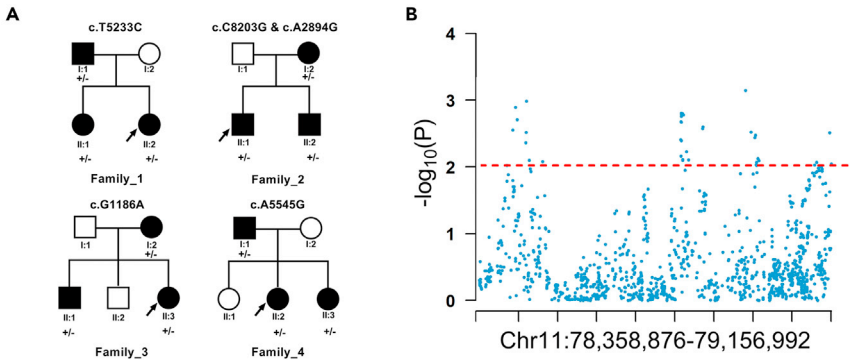

Figure 1. Genetic analysis of *TENM4* in SCZ

(A) *TENM4* rare mutations were identified in four SCZ families, which were p.S1745P in Family_1, p.Q2735E and p.N965S in Family_2, p.V396I in Family_3, and p.T1849A in Family_4.

(B) *TENM4* showed nominally significant association with SCZ according to the previous GWAS.

Ten-m, and *UAS-Ten-m-RNAi*) exhibited courtship suppression after training compared to naive flies. Otherwise, there was no significant difference in CIs between naive and trained experimental flies (*elav > UAS-Ten-m* and *elav > UAS-Ten-m-RNAi*) with *Ten-m* aberrant expression in the nervous system, indicating that pan-neuronal overexpression or downexpression of *Ten-m* lead to lack of the learning ability to suppress courtship behavior (Figure 2A, naive vs trained; *elav-GAL4*, $p < 0.0001$; *UAS-Ten-m*, $p < 0.0001$; *UAS-Ten-m-RNAi*, $p < 0.0001$; *elav > Ten-m*, $p = 0.820$; *elav > Ten-m-RNAi*, $p = 1.000$). In addition, compared with the control groups, flies with aberrantly expressed *Ten-m* pan-neuronally revealed a significant reduction in LIs, which highlighted the courtship STM deficits (Figure 2B, *elav-GAL4* vs *elav > Ten-m*, $p < 0.0001$, *UAS-Ten-m* vs *elav > Ten-m*, $p < 0.0001$; *elav-GAL4* vs *elav > Ten-m-RNAi*, $p < 0.0001$; *UAS-Ten-m-RNAi* vs *elav > Ten-m-RNAi*, $p < 0.0001$). These results suggested that aberrant expression of *Ten-m* in the nervous system impairs STM.

Ten-m affects sleep behavior in *Drosophila*

To determine whether *Ten-m* regulates sleep in *Drosophila*, we increased or decreased *Ten-m* expression levels using transgenes *UAS-Ten-m* and *UAS-Ten-m-RNAi*, respectively, driven by pan-neuronal *elav-GAL4*. Total and

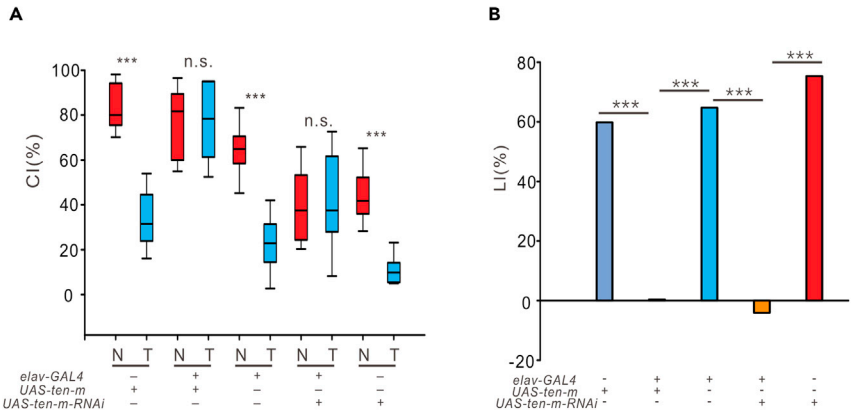

Figure 2. Aberrant expression of *Ten-m* impairs courtship-conditioning learning

(A) CIs of control males (*elav-GAL4*, *UAS-Ten-m*, *UAS-Ten-m-RNAi*, n = 10) and experimental males (*elav > Ten-m* and *elav > Ten-m-RNAi*, n = 10). Box-and-whisker plots of CIs show 10th, 25th, 50th, 75th, and 90th centiles and means (short dashed line). N, naive; T, trained. Experimental males showed no difference in CIs between naive and trained groups, while the CIs of control males in the trained group were significantly lower than in the naive groups.

(B) LIs of control males (*elav-GAL4*, *UAS-Ten-m*, *UAS-Ten-m-RNAi*, n = 10) and experimental males (*elav > Ten-m* and *elav > Ten-m-RNAi*, n = 10). LIs were compared using the permutation test with 100,000 random permutations (one-tail, H1: $LI_{control} > LI_{experimental\ males}$). LIs of experimental males were significantly higher than those in control males.

The Mann-Whitney U test was used for CIs. ***p < 0.001; n.s., no significance.

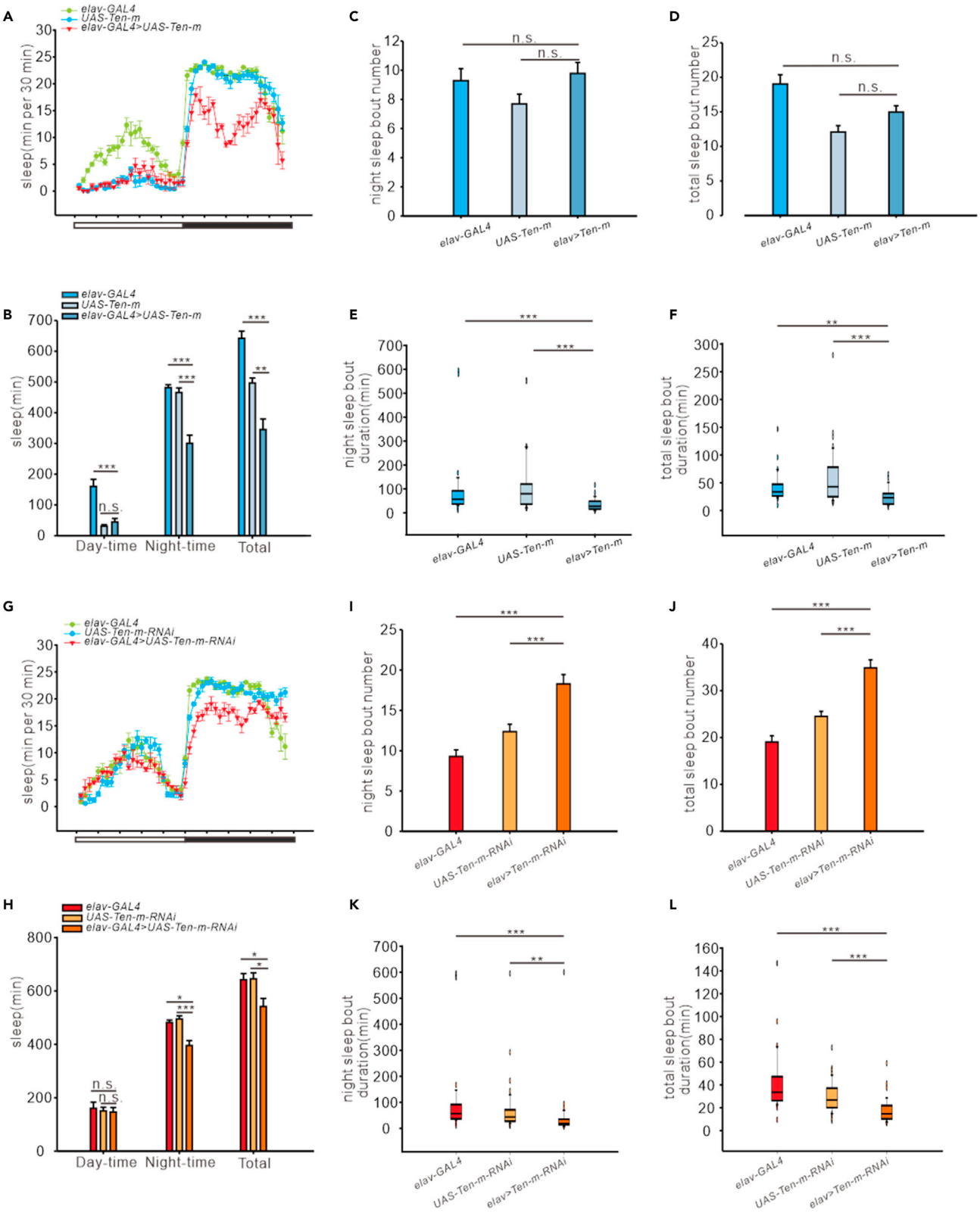
A
elav-GAL4
UAS-Ten-m
elav-GAL4>UAS-Ten-m
sleep(min per 30 min)
B
sleep(min)
n.s.
***
**
Day-time
Night-time
Total
C
night sleep bout number
n.s.
elav-GAL4
UAS-Ten-m
elav>Ten-m
D
total sleep bout number
E
night sleep bout duration(min)
F
total sleep bout duration(min)
G
elav-GAL4
UAS-Ten-m-RNAi
elav-GAL4>UAS-Ten-m-RNAi
sleep(min per 30 min)
H
sleep(min)
I
night sleep bout number
J
total sleep bout number
K
night sleep bout duration(min)
L
total sleep bout duration(min)

Figure 3. Sleep phenotypes in *Ten-m* overexpressed and downexpressed mutants

(A) Conventional sleep plots of controls (*elav-GAL4*, n = 13, *UAS-Ten-m*, n = 16) and experimental flies (*elav* > *Ten-m*, n = 9) in 12-hr LD conditions. White and black bars indicate 12-hr LD periods, respectively.

(B) Total sleep amount (in 24 hr) and sleep during daytime and nighttime in control and experimental flies. Data are represented as mean ± SEM.

(C and D) Histograms of the number of nighttime sleep bouts during nighttime (C) and histograms of the number of total sleep bouts (D) for controls and experimental flies. Data are represented as mean ± SEM.

(E and F) Boxplots of the nighttime sleep bout duration (E) and boxplots of the total sleep bout duration (F) for controls and experimental flies. The line inside the box indicates the median; the upper and lower box limits the 75% and 25% quantiles, respectively; vertical lines above and below the box represent the 90% and 10% quantiles, respectively; points show the 95% and 5% outliers.

(G–L) Conventional sleep plots of controls (*elav-GAL4*, n = 13, and *UAS-Ten-m-RNAi*, n = 14) and experimental flies (*elav* > *Ten-m-RNAi*, n = 13) in 12-hr LD (G). Histograms of total sleep amount and sleep during daytime and nighttime (H), nighttime sleep bout number (I), nighttime sleep bout duration (K), total sleep bout number (J), and total sleep bout duration (L) for controls and experimental flies. Data are represented as mean ± SEM.

One-way analysis of variance (ANOVA) followed by post hoc Tukey were used, except for the comparison of nonparametrically distributed data where the Kruskal-Wallis test was used. *p < 0.05, **p < 0.01, ***p < 0.001; n.s., no significance.

nighttime sleep amounts were decreased both in *elav* > *Ten-m* (Figures 3A and 3B nighttime: *elav-GAL4* vs *elav* > *Ten-m*, p < 0.0001, *UAS-Ten-m* vs *elav* > *Ten-m*, p < 0.0001; total: *elav-GAL4* vs *elav* > *Ten-m*, p < 0.0001; *UAS-Ten-m* vs *elav* > *Ten-m*, p = 0.002) and *elav* > *Ten-m-RNAi* files (Figures 3G and 3H, nighttime: *elav-GAL4* vs *elav* > *Ten-m-RNAi*, p = 0.012; *UAS-Ten-m-RNAi* vs *elav* > *Ten-m-RNAi*, p < 0.0001; total: *elav-GAL4* vs *elav* > *Ten-m-RNAi*, p = 0.019; *UAS-Ten-m-RNAi* vs *elav* > *Ten-m-RNAi*, p = 0.012) compared to controls. In contrast, there was no change in mutants in the daytime sleep of the mutants (Figures 3A and 3B, daytime: *elav-GAL4* vs *elav* > *Ten-m*, p < 0.0001; *UAS-Ten-m* vs *elav* > *Ten-m*, p = 1.000; Figures 3G and 3H, *elav-GAL4* vs *elav* > *Ten-m-RNAi*, p = 0.853; *UAS-Ten-m-RNAi* vs *elav* > *Ten-m-RNAi*, p = 0.986) which might be due to a floor effect, that is, daytime sleep of the controls was minimal. Further analysis revealed that the decreased night and overall sleep in *elav* > *Ten-m* flies was due to the reduced sleep bout duration but not sleep bout number (Figure 3C, *elav-GAL4* vs *elav* > *Ten-m*, p = 0.905, *UAS-Ten-m* vs *elav* > *Ten-m*, p = 0.154; Figure 3D, *elav-GAL4* vs *elav* > *Ten-m*, p = 0.905, *UAS-Ten-m* vs *elav* > *Ten-m*, p = 0.121; Figure 3E, p < 0.0001; Figure 3F, *elav-GAL4* vs *elav* > *Ten-m*, p = 0.005; *UAS-Ten-m* vs *elav* > *Ten-m*, p < 0.0001). These results indicated that over-expressing *Ten-m* in all neurons would impair sleep behavior in *Drosophila* by reducing night sleep bout duration. The night and total sleep bout numbers were significantly increased in *elav* > *Ten-m-RNAi* flies compared to the control groups (Figures 3I and 3J, p < 0.0001). Meanwhile, the night and total sleep bout durations of *elav* > *Ten-m-RNAi* groups were shorter than those of the control groups (Figure 3K, *elav-GAL4* vs *elav* > *Ten-m-RNAi*, p < 0.0001; *UAS-Ten-m-RNAi* vs *elav* > *Ten-m-RNAi*, p = 0.001; Figure 3L, p < 0.0001), suggesting the lack of *Ten-m* impaired sleep maintenance and caused sleep fragmentation in *Drosophila*. Overall, both *Ten-m* overexpression and downexpression impaired sleep maintenance and caused fragmented sleep.

Ten-m affects the aggressive behavior in *Drosophila*

We examined the aggressive behavior of *Ten-m* and *Ten-m-RNAi* flies using different *GAL4* drivers. The latency to initiate fighting was significantly reduced (Figure 4A p < 0.0001; Figure 4B, *elav-GAL4* vs *elav* > *Ten-m-RNAi*, p = 0.009; *UAS-Ten-m-RNAi* vs *elav* > *Ten-m-RNAi*, p < 0.0001), and the frequency was increased (Figure 4A, p < 0.0001; Figure 4B, *elav-GAL4* vs *elav* > *Ten-m-RNAi*, p = 0.832; *UAS-Ten-m-RNAi* vs *elav* > *Ten-m-RNAi*, p = 0.001) in the flies with aberrantly expressed *Ten-m* pan-neuronally compared to the control groups. Male-male aggression is promoted by cVA in *Drosophila* via Or67d and Or65a receptors expressed by ORNs (Wang and Anderson, 2010). ORNs form synapses with PNs and local interneurons (LNs) in the antennal lobe (Das et al., 2008). *Mz699-GAL4* is expressed in 90% of all ventral PNs, and 80% of these *Mz699*-PNs have been identified as GABAergic neurons, which are related to aggression (Lai et al., 2008) (Alekseyenko et al., 2019), and *Mz19* PNs are inherently connected to Or67d ORNs (Hong et al., 2012). We examined the aggressive behavior of *UAS-Ten-m* and *UAS-Ten-m-RNAi* transgenic flies using *Mz699-GAL4*, *Mz19-GAL4*, and *LN1-GAL4*, and latency and frequency changed sharply between the experimental and the control groups (Figures 4A and 4B, p < 0.05, **p < 0.01, ***p < 0.001; n.s., no significance.). These results reveal that aberrant expression of *Ten-m* in *Drosophila* would lead flies to become more aggressive.

RNA sequencing reveals the potential molecular mechanism

Through RNA sequencing of brain tissues in *Drosophila*, differentially expressed genes (DEGs) under the conditions of *Ten-m* overexpression or downexpression were compared (Figure 5A), and the functional classification of these DEGs was carried out. A total of 164 significant DEGs were identified between *elav* > *Ten-m-RNAi* and *elav-GAL4* groups, including 83 upregulated genes and 81 downregulated genes

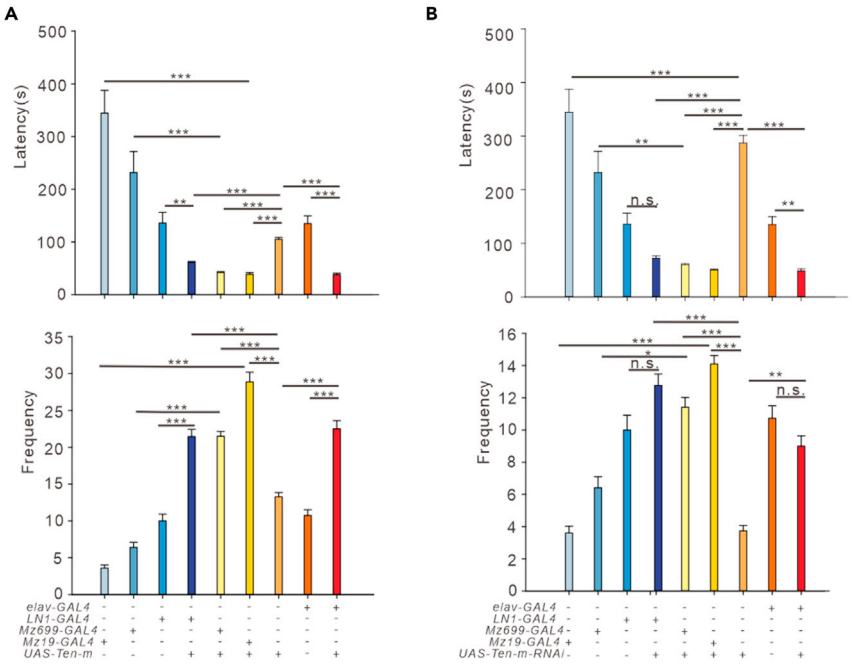

Figure 4. *Ten-m* modulates aggression

(A) The latency and frequency of male flies overexpressing *Ten-m* in all neurons (*elav* > *Ten-m*, n = 14) or in specific neurons such as *Mz699*, *Mz19*, and *LN1* (*Mz699*>*Ten-m*, n = 14, *Mz19*>*Ten-m*, n = 15, *LN1*>*Ten-m*, n = 9) compared to the controls (*elav-GAL4*, n = 15, *UAS-Ten-m*, n = 11, *Mz699-GAL4*, n = 12, *Mz19-GAL4*, n = 10, *LN1-GAL4*, n = 10). Fighting latencies of experimental flies were significantly longer than those in controls, and fighting frequencies of experimental flies were significantly higher than those in controls. Data are represented as mean ± SEM.

(B) The latency and frequency of male flies downexpressing *Ten-m* in all neurons (*elav* > *Ten-m-RNAi*, n = 12) or in specific neurons such as *Mz699*, *Mz19*, and *LN1* (*Mz699*>*Ten-m-RNAi*, n = 12, *Mz19*>*Ten-m-RNAi*, n = 10, *LN1*>*Ten-m-RNAi*, n = 13) compared to the controls (*elav-GAL4*, n = 15, *UAS-Ten-m-RNAi*, n = 11, *Mz699-GAL4*, n = 12, *Mz19-GAL4*, n = 10, *LN1-GAL4*, n = 10). Fighting latencies of experimental flies were significantly longer than those of controls, and fighting frequencies of experimental flies were significantly higher than those of controls. Data are represented as mean ± SEM. One-way ANOVA followed by post hoc Tukey were used, except for the comparison of nonparametrically distributed data where the Kruskal-Wallis test was used. **p < 0.01, ***p < 0.001; n.s., no significance.

(Figure 5B, Table S3). Among DEGs in the *elav* > *Ten-m-RNAi* vs *elav-GAL4*, Gene Ontology (GO) enrichment analysis was related to stimulation, such as biological process (BP) terms linked to response to light stimulus and detection of external stimulus (Figure 5C, Table S5). We also revealed that 130 genes were differentially expressed in *elav* > *Ten-m* vs *elav-GAL4* groups, and 85 genes were upregulated, and 45 genes were downregulated (Figure 5D, Table S2). In the *elav* > *Ten-m* vs *elav-GAL4*, the significantly enriched GO terms were those involved in metabolic processes such as the nucleoside monophosphate metabolic process (Figure 5E, Table S4). As shown in the Venn diagram (Figure 5F), we found there were 55 overlapped DEGs with both overexpressed and decreased expression of *Ten-m*. The clustering heatmap analysis of 55 overlapped significant DEGs indicated a contrasting gene expression profile between experimental groups. *elav* > *Ten-m-RNAi* and *elav* > *Ten-m* had a very similar profile of gene expression, revealing the same high and low expression trends while showing a different profile against *elav-GAL4* (Figure 5G). GO enrichment analysis of overlapped significant DEGs showed that the only BP term was neurogenesis, and the only molecular function (MF) term was ATPase activity (Figure 5H, Table S6).

DISCUSSION

To date, hundreds of genes related to SCZ genes have been identified from GWAS, exome sequencing studies, transcriptomic studies, and epigenetic studies according to the SCZ database (SZDB, http://www.szdb.org/SZDB/index.html) (Sanders and Gill, 2007; Khavari and Cairns, 2020; Xu et al., 2011; Chen et al., 2015; Farrell et al., 2015). Previous studies have also provided amount of evidence for the polygenic architecture of SCZ (Smeland et al., 2020). Many common genetic variants and rare functional mutations make up the polygenic architecture of SCZ (Henriksen et al., 2017). In SCZ, common and rare genetic variants are associated with disorders of

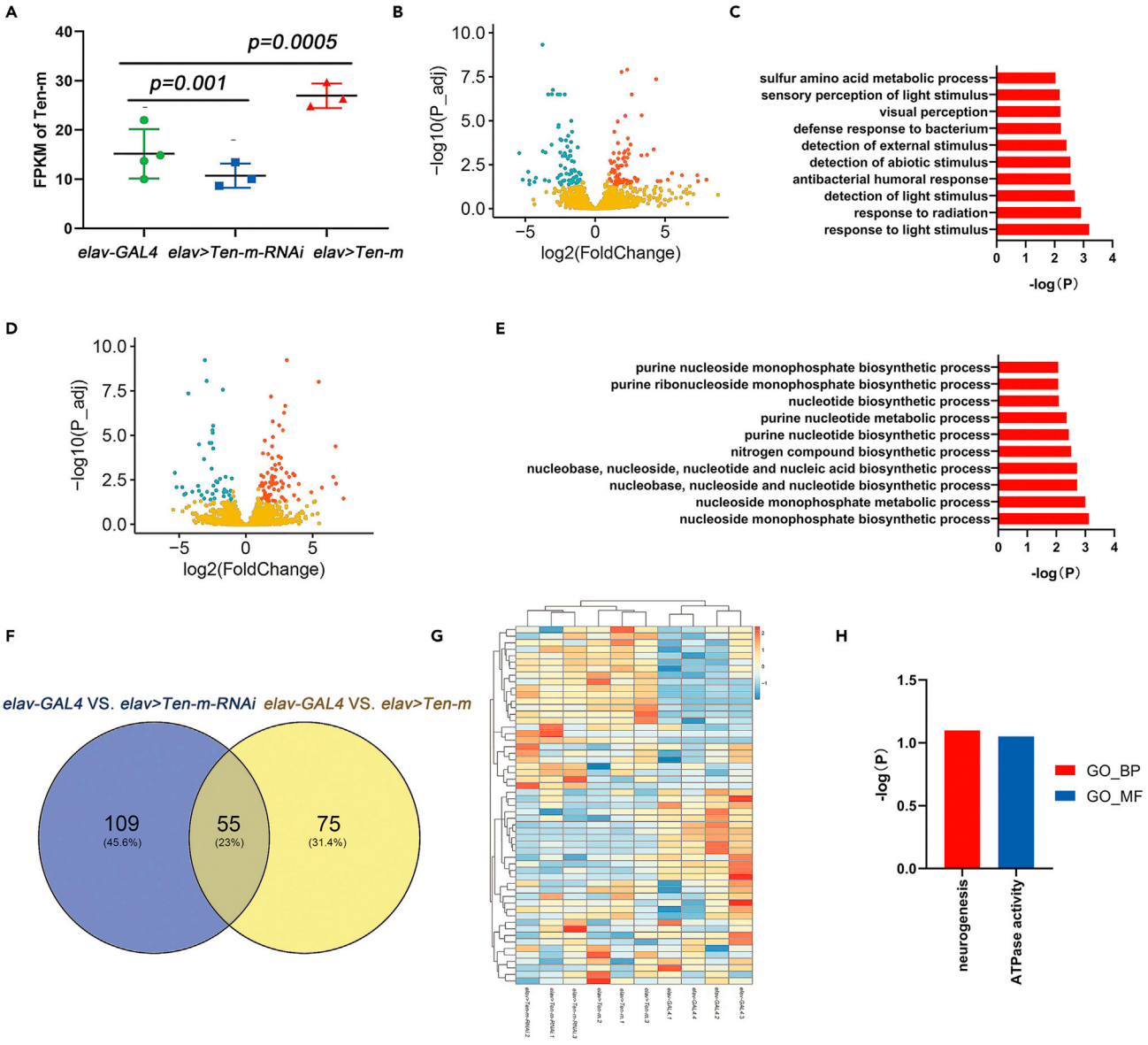

Figure 5. RNA sequencing of brain tissues with aberrant expression of *Ten-m* in *Drosophila*

(A) FPKM of controls (*elav-GAL4*) and experimental flies (*elav > Ten-m* and *elav > Ten-m-RNAi*). Data are represented as mean ± SD. The Kruskal-Wallis test was used for comparison. Compared to the control groups, the experimental groups had increased or decreased the expression of *Ten-m*.

(B) Volcano plots of DEGs from *elav > Ten-m-RNAi* vs *elav-GAL4* groups. Red denotes high expression while blue denotes low expression. In total, 164 significant DEGs were identified, including 83 upregulated genes and 81 downregulated genes.

(C) GO enrichment analysis of DEGs in the *elav > Ten-m-RNAi* group. The DEGs were enriched in stimulation-associated pathways, including light stimulus and detection of external stimulus.

(D) Volcano plots of DEGs from *elav > Ten-m* vs *elav-GAL4* groups. Red denotes high expression while blue denotes low expression. In total, 130 significant DEGs were identified, including 85 upregulated genes and 45 downregulated genes.

(E) GO enrichment analysis of DEGs in the *elav > Ten-m* group. The DEGs were enriched in metabolism-associated pathways, such as the nucleoside monophosphate metabolic process.

(F) Venn diagram showing the intersection of significant DEGs observed in *elav > Ten-m* and *elav > Ten-m-RNAi* groups. There were 55 overlapped DEGs for both decreased and overexpressed *Ten-m*.

(G) Heatmap of overlapped significant DEGs. Hierarchical clustering was performed to highlight the DEGs, indicating a contrasting gene expression profile between experimental groups. Red denotes high expression while blue denotes low expression.

(H) GO enrichment analysis of overlapped significant DEGs in *elav > Ten-m* and *elav > Ten-m-RNAi* groups. The only BP term was neurogenesis, and the only MF term was ATPase activity.

biological processes related to neurodevelopment, neuroexcitability, synaptic function, and the immune system (Ukkola-Vuoti et al., 2019; Boyajyan et al., 2015; Jiang et al., 2020). In this study, we focused on rare functional mutations with minor allele frequency (MAF) < 0.01 in the candidate gene, *TENM4*. We identified five rare functional mutations of *TENM4* gene in SCZ families, suggesting *TENM4* contributes to SCZ. Interestingly, common SNPs in *TENM4* only presented a nominally significant association with SCZ and did not reach the level of genome-wide significance, which might be because most mutations identified in *TENM4* were missense mutations. Unlike the loss of function mutations, most missense mutations have a reduced effect on gene function, and some mutations might even not affect gene function. It is not easily to distinguish these mutations from the true functional missense mutations, but the GWAS results revealed that there might still be a genetic influence of *TENM4* on SCZ. We have not performed the sequencing in patients with sporadic SCZ because the limited sample size would affect the results a lot, and the very big sample size may find the association between rare functional mutations.

TENM4 is known to be involved in mental illness and cognition, but there has been no behavioral analysis of *TENM4* in animal models. Thus, we used the *Drosophila* model to demonstrate the potential mechanism of SCZ caused by *TENM4* mutations. We observed reduced STM with abnormal neuronal expression of *Ten-m*. Intellectual disability and learning disabilities are prevalent in patients with SCZ. SCZ is also associated with a substantial cognitive impairment that affects working memory, processing speed, attention, and verbal memory (Dickinson et al., 2007). It is also difficult for patients with SCZ to learn from positive feedback (Dowd and Barch, 2012). Patients with SCZ often reveal social withdrawal, and the possibility of violence is increased (Lamberti, 2007). Sleep and circadian rhythm disorders occur in many psychiatric patients, including SCZ (Wulff et al., 2010). Furthermore, sleep disturbances occur frequently in patients with SCZ (Cohrs, 2008), including shorter duration, sleep fragmentation, insomnia, or other sleeping disorders (Monti and Monti, 2004). We found that the aberrant expression of *Ten-m* could cause sleep reduction and increased aggressiveness, which exhibit an SCZ-like phenotype. Thus, we inferred that *TENM4* is a promising candidate gene, which might be related to some SCZ symptoms in SCZ, such as high aggression levels, sleep disorders, and learning ability related to cognitive deficits.

Overexpression and downexpression of *Ten-m* both caused night-sleep reduction in *Drosophila*, but the effect was not the same. Overexpression of *Ten-m* caused reduced sleep duration, and both overexpression and downexpression of *Ten-m* caused sleep fragmentation. We speculated that these effects were caused by different mechanisms, which need to be studied. The GWAS of actigraphic sleep phenotypes indicated that wake after sleep onset is associated with *TENM4* (Spada et al., 2016).

SCZ is related to severe abnormal mutations in genes essential for synaptic plasticity (Gulsuner et al., 2020). Neural circuits of the human brain are composed of approximately 100 million neurons intercommunicated by synapses which are eventually responsible for behavior and brain function (Li et al., 2016). *Ten-m* affects the synapses morphological structure in *Drosophila*, suggesting that the aberrant expression of *TENM4* may cause changes in synapse morphological structure which could lead to SCZ.

RNA sequencing showed that the effect of *Ten-m* on stimulation and the metabolic process might cause behavioral abnormalities. The sensitivity to cVA in males plays an important role in learning, memory, and aggressive behavior, while the sensory perception of light stimulation affects sleep in *Drosophila*. In addition, the imbalance of the nucleoside pathway and metabolism significantly affects the neuromodulatory function significantly (Ipata et al., 2011). The GO enrichment analysis of overlapped significant DEGs revealed neurogenesis and ATPase activity. Moreover, hippocampal neurogenesis and synaptic functions are crucial for learning and memory (Nabavi et al., 2014). Aberrant subcortical neurogenesis often occurs in SCZ (Hoffmann et al., 2019). The abnormal regulation of energy metabolism leads to changes in the synthesis and release of ATP. Studies have shown that ATP is the main stimulant of microglial and can be used as a signal to mediate the growth of microglial and the communication of nerve cells, which would affect the function of neurons and synapses (Davalos et al., 2005). Thus, the molecular mechanism of *TENM4* on SCZ might be mainly through affecting neurogenesis and regulating ATPase activity.

Limitations of the study

There are still some limitations in our study. For example, we need a big sample size of sporadic SCZ patients to perform the target sequencing to find the association between rare functional mutations. More functional experiments should be set to find more direct pathological evidence in SCZ. The molecular mechanism of *TENM4* on SCZ remains unclear.

STAR★METHODS

Detailed methods are provided in the online version of this paper and include the following:

- KEY RESOURCES TABLE
- RESOURCE AVAILABILITY
  - Lead contact
  - Materials availability
  - Data and code availability
- EXPERIMENTAL MODEL AND SUBJECT DETAILS
  - Patients and samples
  - Fly lines
- METHOD DETAILS
  - Targeted sequencing of *TENM4*
  - Courtship conditioning assay
  - Aggression assay
  - Sleep and activity assay
  - RNA extraction and sequencing
- QUANTIFICATION AND STATISTICAL ANALYSIS

SUPPLEMENTAL INFORMATION

Supplemental information can be found online at https://doi.org/10.1016/j.isci.2021.103063.

ACKNOWLEDGMENTS

We acknowledge the altruism of the participants and their families and support staff at each of the participating sites for their contributions to this study. This work was supported by grants from the National Key Research and Development Program (2016YFC0906400 and 2016YFC1201700), the National Natural Science Foundation of China (grant 8142106, 81970999, 82071262 and 81872297), Innovation Funding in Shanghai (20JC1418600), the Shanghai Leading Academic Discipline Project (B205), and Shanghai Rising-Star Program (19QA1404900).

AUTHOR CONTRIBUTIONS

D.Z., Y.P., G.H., and L.H. designed the study and interpreted the results. X.L., D.C., L.W., X.W., F.Y., and X.C. collected the samples and performed the primary experiments. X.Y. and H.D. conducted targeted sequencing, and D.Z. performed statistical analysis. X.Y. and M.L. performed the animal experiments. X.Y. and D.Z. performed the RNA-seq and GO analysis. D.Z., Y.P., X.Y., and M.L. verified the underlying data. X.Y. and M.L. drafted the manuscript, and all authors contributed to the final version of the paper.

DECLARATION OF INTERESTS

The authors declare no competing interests.

Received: February 8, 2021
Revised: June 23, 2021
Accepted: August 26, 2021
Published: September 24, 2021

REFERENCES

Alekseyenko, O.V., Chan, Y.B., Okaty, B.W., Chang, Y., Dymecki, S.M., and Kravitz, E.A. (2019). Serotonergic modulation of aggression in Drosophila involves GABAergic and cholinergic opposing pathways. Curr. Biol. *29*, 2145–2156 e5.

Anders, S., Pyl, P.T., and Huber, W. (2015). HTSeq–a Python framework to work with high-throughput sequencing data. Bioinformatics *31*, 166–169.

Baumgartner, S., Martin, D., Hagios, C., and Chiquet-Ehrismann, R. (1994). Tenm, a Drosophila gene related to tenascin, is a new pair-rule gene. EMBO J. *13*, 3728–3740.

Bolger, A.M., Lohse, M., and Usadel, B. (2014). Trimmomatic: a flexible trimmer for Illumina sequence data. Bioinformatics *30*, 2114–2120.

Boyajyan, A., Zakharyan, R., Atshemyan, S., Chavushyan, A., and Mkrtchyan, G. (2015). Schizophrenia-associated risk and protective variants of c-Fos encoding gene. Recent Adv. DNA Gene Seq. *9*, 51–57.

Chao, Y.X., Lin Ng, E.Y., Tio, M., Kumar, P., Tan, L., Au, W.L., Yih, Y., and Tan, E.K. (2016). Essential tremor linked TENM4 mutation found in healthy Chinese individuals. Parkinsonism Relat. Disord. *31*, 139–140.

Chen, J., Cao, F., Liu, L., Wang, L., and Chen, X. (2015). Genetic studies of schizophrenia: an update. Neurosci. Bull. *31*, 87–98.

Chen, S., Lee, A.Y., Bowens, N.M., Huber, R., and Kravitz, E.A. (2002). Fighting fruit flies: a model

system for the study of aggression. Proc. Natl. Acad. Sci. U S A *99*, 5664–5668.

Cohrs, S. (2008). Sleep disturbances in patients with schizophrenia : impact and effect of antipsychotics. CNS Drugs *22*, 939–962.

Das, A., Sen, S., Lichtneckert, R., Okada, R., Ito, K., Rodrigues, V., and Reichert, H. (2008). Drosophila olfactory local interneurons and projection neurons derive from a common neuroblast lineage specified by the empty spiracles gene. Neural Dev. *3*, 33.

Davalos, D., Grutzendler, J., Yang, G., Kim, J.V., Zuo, Y., Jung, S., Littman, D.R., Dustin, M.L., and Gan, W.B. (2005). ATP mediates rapid microglial response to local brain injury in vivo. Nat. Neurosci. *8*, 752–758.

Dickinson, D., Ramsey, M.E., and Gold, J.M. (2007). Overlooking the obvious: a meta-analytic comparison of digit symbol coding tasks and other cognitive measures in schizophrenia. Arch. Gen. Psychiatry *64*, 532–542.

Dowd, E.C., and Barch, D.M. (2012). Pavlovian reward prediction and receipt in schizophrenia: relationship to anhedonia. PLoS One *7*, e35622.

Everaerts, C., Farine, J.P., Cobb, M., and Ferveur, J.F. (2010). Drosophila cuticular hydrocarbons revisited: mating status alters cuticular profiles. PLoS One *5*, e9607.

Farrell, M.S., Werge, T., Sklar, P., Owen, M.J., Ophoff, R.A., O'donovan, M.C., Corvin, A., Cichon, S., and Sullivan, P.F. (2015). Evaluating historical candidate genes for schizophrenia. Mol. Psychiatry *20*, 555–562.

Feng, K., Zhou, X.H., Oohashi, T., Morgelin, M., Lustig, A., Hirakawa, S., Ninomiya, Y., Engel, J., Rauch, U., and Fassler, R. (2002). All four members of the Ten-m/Odz family of transmembrane proteins form dimers. J. Biol. Chem. *277*, 26128–26135.

Forshew, T., Murtaza, M., Parkinson, C., Gale, D., Tsui, D.W., Kaper, F., Dawson, S.J., Piskorz, A.M., Jimenez-Linan, M., Bentley, D., et al. (2012). Noninvasive identification and monitoring of cancer mutations by targeted deep sequencing of plasma DNA. Sci. Transl. Med. *4*, 136ra68.

Gulsuner, S., Stein, D.J., Susser, E.S., Sibeko, G., Pretorius, A., Walsh, T., Majara, L., Mndini, M.M., Mqulwana, S.G., Ntola, O.A., et al. (2020). Genetics of schizophrenia in the South African Xhosa. Science *367*, 569–573.

Heinrich, A., Lourdusamy, A., Tzschoppe, J., Vollstadt-Klein, S., Buhler, M., Steiner, S., Bach, C., Poustka, L., Banaschewski, T., Barker, G., et al. (2013). The risk variant in ODZ4 for bipolar disorder impacts on amygdala activation during reward processing. Bipolar Disord. *15*, 440–445.

Henriksen, M.G., Nordgaard, J., and Jansson, L.B. (2017). Genetics of schizophrenia: overview of methods, findings and limitations. Front. Hum. Neurosci. *11*, 322.

Hoffmann, A., Ziller, M., and Spengler, D. (2019). Progress in iPSC-based modeling of psychiatric disorders. Int. J. Mol. Sci. *20*, 4896.

Hong, W., Mosca, T.J., and Luo, L. (2012). Teneurins instruct synaptic partner matching in an olfactory map. Nature *484*, 201–207.

Hor, H., Francescatto, L., Bartesaghi, L., Ortega-Cubero, S., Kousi, M., Lorenzo-Betancor, O., Jimenez-Jimenez, F.J., Gironell, A., Clarimon, J., Drechsel, O., et al. (2015). Missense mutations in TENM4, a regulator of axon guidance and central myelination, cause essential tremor. Hum. Mol. Genet. *24*, 5677–5686.

Ikeda, M., Takahashi, A., Kamatani, Y., Okahisa, Y., Kunugi, H., Mori, N., Sasaki, T., Ohmori, T., Okamoto, Y., Kawasaki, H., et al. (2018). A genome-wide association study identifies two novel susceptibility loci and trans population polygenicity associated with bipolar disorder. Mol. Psychiatry *23*, 639–647.

Iossifov, I., O'roak, B.J., Sanders, S.J., Ronemus, M., Krumm, N., Levy, D., Stessman, H.A., Witherspoon, K.T., Vives, L., Patterson, K.E., et al. (2014). The contribution of de novo coding mutations to autism spectrum disorder. Nature *515*, 216–221.

Ipata, P.L., Camici, M., Micheli, V., and Tozz, M.G. (2011). Metabolic network of nucleosides in the brain. Curr. Top Med. Chem. *11*, 909–922.

Ivorra, J.L., Rivero, O., Costas, J., Iniesta, R., Arrojo, M., Ramos-Rios, R., Carracedo, A., Palomo, T., Rodriguez-Jimenez, R., Cervilla, J., et al. (2014). Replication of previous genome-wide association studies of psychiatric diseases in a large schizophrenia case-control sample from Spain. Schizophr. Res. *159*, 107–113.

Jiang, S., Zhou, D., Wang, Y.Y., Jia, P., Wan, C., Li, X., He, G., Cao, D., Jiang, X., Kendler, K.S., et al. (2020). Identification of de novo mutations in prenatal neurodevelopment-associated genes in schizophrenia in two Han Chinese patient-sibling family-based cohorts. Transl. Psychiatry *10*, 307.

Kavanagh, D.H., Tansey, K.E., O'donovan, M.C., and Owen, M.J. (2015). Schizophrenia genetics: emerging themes for a complex disorder. Mol. Psychiatry *20*, 72–76.

Keleman, K., Vrontou, E., Kruttner, S., Yu, J.Y., Kurtovic-Kozaric, A., and Dickson, B.J. (2012). Dopamine neurons modulate pheromone responses in Drosophila courtship learning. Nature *489*, 145–149.

Khavari, B., and Cairns, M.J. (2020). Epigenomic dysregulation in schizophrenia: in search of disease etiology and biomarkers. Cells *9*, 1837.

Kim, D., Pertea, G., Trapnell, C., Pimentel, H., Kelley, R., and Salzberg, S.L. (2013). TopHat2: accurate alignment of transcriptomes in the presence of insertions, deletions and gene fusions. Genome Biol. *14*, R36.

Lai, S.L., Awasaki, T., Ito, K., and Lee, T. (2008). Clonal analysis of Drosophila antennal lobe neurons: diverse neuronal architectures in the lateral neuroblast lineage. Development *135*, 2883–2893.

Lam, M., Chen, C.Y., Li, Z., Martin, A.R., Bryois, J., Ma, X., Gaspar, H., Ikeda, M., Benyamin, B., Brown, B.C., et al. (2019). Comparative genetic architectures of schizophrenia in East Asian and European populations. Nat. Genet. *51*, 1670–1678.

Lamberti, J.S. (2007). Understanding and preventing criminal recidivism among adults with psychotic disorders. Psychiatr. Serv. *58*, 773–781.

Langmead, B., and Salzberg, S.L. (2012). Fast gapped-read alignment with Bowtie 2. Nat. Methods *9*, 357–359.

Li, H., and Durbin, R. (2009). Fast and accurate short read alignment with Burrows-Wheeler transform. Bioinformatics *25*, 1754–1760.

Li, H., Handsaker, B., Wysoker, A., Fennell, T., Ruan, J., Homer, N., Marth, G., Abecasis, G., Durbin, R., and Genome Project Data Processing, S. (2009). The sequence alignment/map format and SAMtools. Bioinformatics *25*, 2078–2079.

Li, J., Wilkinson, B., Clementel, V.A., Hou, J., O'dell, T.J., and Coba, M.P. (2016). Long-term potentiation modulates synaptic phosphorylation networks and reshapes the structure of the postsynaptic interactome. Sci. Signal. *9*, rs8.

Li, Z., Chen, J., Yu, H., He, L., Xu, Y., Zhang, D., Yi, Q., Li, C., Li, X., Shen, J., et al. (2017). Genome-wide association analysis identifies 30 new susceptibility loci for schizophrenia. Nat. Genet. *49*, 1576–1583.

Love, M.I., Huber, W., and Anders, S. (2014). Moderated estimation of fold change and dispersion for RNA-seq data with DESeq2. Genome Biol. *15*, 550.

McKenna, A., Hanna, M., Banks, E., Sivachenko, A., Cibulskis, K., Kernytsky, A., Garimella, K., Altshuler, D., Gabriel, S., Daly, M., and Depristo, M.A. (2010). The Genome Analysis Toolkit: a MapReduce framework for analyzing next-generation DNA sequencing data. Genome Res. *20*, 1297–1303.

Monti, J.M., and Monti, D. (2004). Sleep in schizophrenia patients and the effects of antipsychotic drugs. Sleep Med. Rev. *8*, 133–148.

Mosca, T.J., Hong, W., Dani, V.S., Favaloro, V., and Luo, L. (2012). Trans-synaptic Teneurin signalling in neuromuscular synapse organization and target choice. Nature *484*, 237–241.

Nabavi, S., Fox, R., Proulx, C.D., Lin, J.Y., Tsien, R.Y., and Malinow, R. (2014). Engineering a memory with LTD and LTP. Nature *511*, 348–352.

Patel, K.R., Cherian, J., Gohil, K., and Atkinson, D. (2014). Schizophrenia: overview and treatment options. P T *39*, 638–645.

Psychiatric GWAS Consortium Bipolar Disorder Working Group (2011). Large-scale genome-wide association analysis of bipolar disorder identifies a new susceptibility locus near ODZ4. Nat. Genet. *43*, 977–983.

Robinson, J.T., Thorvaldsdottir, H., Winckler, W., Guttman, M., Lander, E.S., Getz, G., and Mesirov, J.P. (2011). Integrative genomics viewer. Nat. Biotechnol. *29*, 24–26.

Sanders, J., and Gill, M. (2007). Unravelling the genome: a review of molecular genetic research in schizophrenia. Ir. J. Med. Sci. *176*, 5–9.

Siegel, R.W., and Hall, J.C. (1979). Conditioned responses in courtship behavior of normal and mutant Drosophila. Proc. Natl. Acad. Sci. U S A *76*, 3430–3434.

Siwicki, K.K., Riccio, P., Ladewski, L., Marcillac, F., Dartevelle, L., Cross, S.A., and Ferveur, J.F. (2005). The role of cuticular pheromones in courtship conditioning of Drosophila males. Learn Mem. *12*, 636–645.

Smeland, O.B., Frei, O., Dale, A.M., and Andreassen, O.A. (2020). The polygenic architecture of schizophrenia - rethinking pathogenesis and nosology. Nat. Rev. Neurol. *16*, 366–379.

Song, Q., Feng, G., Huang, Z., Chen, X., Chen, Z., and Ping, Y. (2017). Aberrant axonal arborization of PDF neurons induced by abeta42-mediated JNK activation underlies sleep disturbance in an Alzheimer's model. Mol. Neurobiol. *54*, 6317–6328.

Spada, J., Scholz, M., Kirsten, H., Hensch, T., Horn, K., Jawinski, P., Ulke, C., Burkhardt, R., Wirkner, K., Loeffler, M., et al. (2016). Genome-wide association analysis of actigraphic sleep phenotypes in the LIFE Adult Study. J. Sleep Res. *25*, 690–701.

Sullivan, P.F., Daly, M.J., and O'donovan, M. (2012). Genetic architectures of psychiatric disorders: the emerging picture and its implications. Nat. Rev. Genet. *13*, 537–551.

Suzuki, N., Fukushi, M., Kosaki, K., Doyle, A.D., De Vega, S., Yoshizaki, K., Akazawa, C., Arikawa-Hirasawa, E., and Yamada, Y. (2012). Teneurin-4 is a novel regulator of oligodendrocyte differentiation and myelination of small-diameter axons in the CNS. J. Neurosci. *32*, 11586–11599.

Suzuki, N., Numakawa, T., Chou, J., De Vega, S., Mizuniwa, C., Sekimoto, K., Adachi, N., Kunugi, H., Arikawa-Hirasawa, E., Yamada, Y., and Akazawa, C. (2014). Teneurin-4 promotes cellular protrusion formation and neurite outgrowth through focal adhesion kinase signaling. FASEB J. *28*, 1386–1397.

Trapnell, C., Roberts, A., Goff, L., Pertea, G., Kim, D., Kelley, D.R., Pimentel, H., Salzberg, S.L., Rinn, J.L., and Pachter, L. (2012). Differential gene and transcript expression analysis of RNA-seq experiments with TopHat and Cufflinks. Nat. Protoc. *7*, 562–578.

Tucker, R.P., and Chiquet-Ehrismann, R. (2006). Teneurins: a conserved family of transmembrane proteins involved in intercellular signaling during development. Dev. Biol. *290*, 237–245.

Tucker, R.P., Martin, D., Kos, R., and Chiquet-Ehrismann, R. (2000). The expression of teneurin-4 in the avian embryo. Mech. Dev. *98*, 187–191.

Ukkola-Vuoti, L., Torniainen-Holm, M., Ortega-Alonso, A., Sinha, V., Tuulio-Henriksson, A., Paunio, T., Lonnqvist, J., Suvisaari, J., and Hennah, W. (2019). Gene expression changes related to immune processes associate with cognitive endophenotypes of schizophrenia. Prog. Neuropsychopharmacol. Biol. Psychiatry *88*, 159–167.

Untergasser, A., Cutcutache, I., Koressaar, T., Ye, J., Faircloth, B.C., Remm, M., and Rozen, S.G. (2012). Primer3–new capabilities and interfaces. Nucleic Acids Res. *40*, e115.

Wang, K., Li, M., and Hakonarson, H. (2010). ANNOVAR: functional annotation of genetic variants from high-throughput sequencing data. Nucleic Acids Res. *38*, e164.

Wang, L., and Anderson, D.J. (2010). Identification of an aggression-promoting pheromone and its receptor neurons in Drosophila. Nature *463*, 227–231.

Wu, H., Zhou, D.Z., Berki, D., Geisz, A., Zou, W.B., Sun, X.T., Hu, L.H., Zhao, Z.H., Zhao, A.J., He, L., et al. (2017). No significant enrichment of rare functionally defective CPA1 variants in a large Chinese idiopathic chronic pancreatitis cohort. Hum. Mutat. *38*, 959–963.

Wulff, K., Gatti, S., Wettstein, J.G., and Foster, R.G. (2010). Sleep and circadian rhythm disruption in psychiatric and neurodegenerative disease. Nat. Rev. Neurosci. *11*, 589–599.

Xu, B., Roos, J.L., Dexheimer, P., Boone, B., Plummer, B., Levy, S., Gogos, J.A., and Karayiorgou, M. (2011). Exome sequencing supports a de novo mutational paradigm for schizophrenia. Nat. Genet. *43*, 864–868.

Xue, C.B., Xu, Z.H., Zhu, J., Wu, Y., Zhuang, X.H., Chen, Q.L., Wu, C.R., Hu, J.T., Zhou, H.S., Xie, W.H., et al. (2018). Exome sequencing identifies TENM4 as a novel candidate gene for schizophrenia in the SCZD2 locus at 11q14-21. Front. Genet. *9*, 725.

Yan, Y.P., Xu, C.Y., Gu, L.Y., Zhang, B., Shen, T., Gao, T., Tian, J., Pu, J.L., Yin, X.Z., Zhang, B.R., and Zhao, G.H. (2020). Genetic testing of FUS, HTRA2, and TENM4 genes in Chinese patients with essential tremor. CNS Neurosci. Ther. *26*, 837–841.

Zhou, C., Rao, Y., and Rao, Y. (2008). A subset of octopaminergic neurons are important for Drosophila aggression. Nat. Neurosci. *11*, 1059–1067.

Zhou, X.H., Brandau, O., Feng, K., Oohashi, T., Ninomiya, Y., Rauch, U., and Fassler, R. (2003). The murine Ten-m/Odz genes show distinct but overlapping expression patterns during development and in adult brain. Gene Expr. Patterns *3*, 397–405.

STAR★METHODS

KEY RESOURCES TABLE

REAGENT or RESOURCE	SOURCE	IDENTIFIER
Biological samples		
Human blood	SJTU BIO-X psychiatric sample bank	http://www.bio-x.cn/
Deposited data		
Raw data of Target sequencing	This paper	Mendeley Data, V2, https://doi.org/10.17632/6w5zmn6j8h.2.
mRNA sequencing analyzed data	This paper	Mendeley Data, V1, https://doi.org/10.17632/hy3bh2z8x8.1
Experimental models: Organisms/strains		
D. melanogaster: *elav-GAL4*	Bloomington Drosophila Stock Center	flybase_FBst0000458
D. melanogaster: *Mz19-GAL4*	Bloomington Drosophila Stock Center	flybase_FBal0155865
D. melanogaster: *Mz699-GAL4*	Bloomington Drosophila Stock Center	flybase_FBal0066073
D. melanogaster: *UAS-Ten-m*	Bloomington Drosophila Stock Center	flybase_FBst0041569
D. melanogaster: *UAS-Ten-m-RNAi*	Bloomington Drosophila Stock Center	flybase_FBtp0052660
D. melanogaster: *w;Cyo/sco;MKRS/Tb*	Kyoto Stock Center	flybase_FBst0305835
D. melanogaster: *LN1-GAL4*	Kyoto Stock Center	flybase_FBst0302813
Oligonucleotides		
Primers for *TENM4*, see supplemental information Such as: GACCCTGTTTGT GGATGTGGA	This paper	N/A
Software and algorithms		
Burrows-Wheeler Aligner (BWA)	Li and Durbin, 2009	http://bio-bwa.sourceforge.net/
Samtools	Li et al. (2009)	http://samtools.sourceforge.net/
Genome Analysis Toolkit (GATK)	McKenna et al. (2010)	http://www.broadinstitute.org/gsa/wiki/index.php/The_Genome_Analysis_Toolkit
ANNOVAR	Wang et al. (2010)	https://annovar.openbioinformatics.org/en/latest/
IGV	Robinson et al. (2011)	http://www.igv.org/
Trimmomatic	Bolger et al. (2014)	http://www.usadellab.org/cms/index.php?page=trimmomatic
TopHat2	Kim et al. (2013)	http://ccb.jhu.edu/software/tophat/manual.shtml
Cufflinks	Trapnell et al. (2012)	http://cole-trapnell-lab.github.io/cufflinks/
Bowtie2	Langmead and Salzberg (2012)	http://bowtie-bio.sourceforge.net/bowtie2/index.shtml
HTSeq	Anders et al. (2015)	https://htseq.readthedocs.io/en/master/
DESeq2	Love et al. (2014)	http://bioconductor.org/packages/release/bioc/html/DESeq2.html

RESOURCE AVAILABILITY

Lead contact

Further information and requests for resources and reagents should be directed to and will be fulfilled by the Lead Contact, Daizhan Zhou (zhoudaizhan@sjtu.edu.cn).

Materials availability

Materials used or generated in this study will be available upon reasonable request, and a material transfer agreement may be required.

Data and code availability

The target sequencing data of *TENM4* and the RNA sequencing data have been deposited at Mendeley Data and are publicly available as of the date of publication. Accession numbers are listed in the key resources table.

This paper does not report original code.

Any additional information required to reanalyze the data reported in this paper is available from the lead contact upon request.

EXPERIMENTAL MODEL AND SUBJECT DETAILS

Patients and samples

In this study, all individuals with SCZ were interviewed by at least two independent psychiatrists. Diagnoses were made strictly according to the Diagnostic and Statistical Manual of Mental Disorders (DSM)-IV criteria, and patients with other neurological, mental, or psychiatric disorders, or with history of drug use were excluded. All participants provided written informed consent. Approval for our study was received from the Ethics Committee of Human Genetic Resources of Shanghai Jiao Tong University and local hospitals.

For the family-based sequencing study, 68 SCZ families with no less than 3 patients each were selected, and 351 samples were collected for targeted sequencing. There are 183 males and 168 females, and the average age was 39. All blood samples were collected during 1998-2005 in Shanghai, Shandong, Hebei, Anhui, Gansu, Heilongjiang and Guangxi provinces in China.

Fly lines

The fly lines used can be found in Table S1. Other genotypes were obtained by fly crossing. All procedures were approved by the Ethics Committee of Animal Research of Shanghai Jiao Tong University.

The larvae and adults were kept on a standard sugar-yeast-cornmeal medium under a 12-hour light/dark (LD) cycle at 25°C with 60% humidity. A list of fly lines used can be found in Table S1. Two genotypes of fly stocks were obtained by crossing other genotypes, *elav>Ten-m* and *elav>Ten-m-RNAi*. We used balanced lethal genotype flies: *w;Cyo/sco;MKRS/Tb*. The genotype includes four types of lethal alleles, which cause the death of the organism that carries them. To obtain *elav>Ten-m* flies, firstly, *UAS-Ten-m* flies were crossed with *w;Cyo/sco;MKRS/Tb* flies. We selected presenting *Cyo* and *MKRS* phenotypes of male flies from the offspring to cross with female *elav;+;+* flies, then selected *elav;Cyo/+;UAS-Ten-m/+* males. Simultaneously, female *elav;+;+* flies were crossed with *w;Cyo/sco;MKRS/Tb* flies, and we selected presenting *Cyo* and *MKRS* phenotypes of male flies from the offspring to cross with female *elav;+;+* flies, then selected *elav;Cyo/+;MKRS/+* females to cross with the *elav;Cyo/+;UAS-Ten-m/+* males. Finally, we obtained *elav>Ten-m* flies. The same methods were used to obtain *elav>Ten-m-RNAi* flies. Other fly genotypes were obtained by crossing parental flies. More than five generations with the w^{1118} strain outcrossing were performed to standardize the background.

In crossing experiment, we used 20 mature females and 10 mature males. In courtship conditioning assay, we used 10 males and 10 females which were selected at the eclosion stage. In aggression assay, we used only males which were kept separately for 7 days after eclosion stage. In sleep and activity assay, we used only virgin females which were collected immediately after eclosion stage.

METHOD DETAILS

Targeted sequencing of *TENM4*

Primer3 was used to design 70 target-specific primer pairs for all exons and exon-intron boundaries of *TENM4* (Untergasser et al., 2012). The primers were synthesized with common adapter sequences at their 5′ ends as previously described (Forshew et al., 2012). All 70 primer pairs were divided into 6 multiplex

primer pools. The library construction was performed essentially as previously described, including pre-amplification of the tagged gene amplicons, generation of a barcoded DNA library, quantification and clean-up (Forshew et al., 2012). The final DNA libraries were determined by Qubit 2100 (Thermo Scientific, USA) and Bioanalyzer (Illumina, USA) and then sequenced on the Illumina HiSeq X-Ten System (Illumina, USA) (Wu et al., 2017).

The targeted next-generation sequencing data were filtered by quality analysis and PCR primers and splices, and the paired 150 bp-long reads were mapped to hg19 human reference genome using the Burrows-Wheeler Aligner (BWA) software (Li and Durbin, 2009). Samtools was used for sequence sorting, gene location labeling, and format transformation (Li et al., 2009). Genome Analysis Toolkit (GATK) was used to identify mutation, filter and select comment to generate a VCF file (McKenna et al., 2010) . All variants were annotated by ANNOVAR software (2019Oct24) (Wang et al., 2010), and the potential effects on the protein function were predicted using 9 software (SIFT, PolyPhen2, LRT, MutationTaster, MutationAssessor, FATHMM, PROVEAN, MetaSVM, and MetaLR). All functional mutations were visually confirmed one-by-one using IGV software (v2.8.6) (Robinson et al., 2011).

Courtship conditioning assay

A courtship conditioning assay was used to test courtship behavior and learning memory in *Drosophila*. Males and females were selected at the eclosion stage and raised in *Drosophila* standard culture medium. Male flies were kept separately and females were kept in groups of 10-15 flies. Before the experiments, selected females were pre-mated by housing with 15-20 w^{1118} males per group for 18 hours. Males were divided into naive group and trained group. Male flies in trained groups aged up to 4-7 days after eclosion were solely paired with two mated females 1h for training, then the mated females were removed for half an hour before the test. Individual males from the control or trained groups were placed into the test chamber, 15 mm in diameter by 7 mm deep, and paired with two mated females. The period of experiments lasted for 10 minutes and were recorded by a video camera. The courtship index (CI) was calculated as the percentage of male courtship duration within 10 minutes. The learning index (LI) was calculated using the mean CIs, $LI = [CI_{naive} - CI_{trained}]/CI_{naive}$ (Keleman et al., 2012). As the distributions of LIs are different between groups, LIs were used for the permutation test with 100,000 random permutations to compare between groups, and the data were processed with R software. One-tail testing against the null hypothesis was used in the comparison. The Mann–Whitney U test was used for CIs.

Aggression assay

Pairs of male flies were introduced into a fighting chamber, which was 13 mm in diameter by 7 mm in height. We used 20 mm × 20 mm glass slides to cover the chamber. Fly behaviors were observed and recorded for 15 minutes (Zhou et al., 2008).The aggressive behaviors of male flies were evaluated in two aspects: latency and frequency. Latency is the duration between putting experimental flies into the chambers and the start of the first agonistic encounter while frequency is the number of aggressive behaviors of male flies, such as lunges, within 15 minutes. (Chen et al., 2002).

Sleep and activity assay

All experimental flies were virgin females collected immediately after eclosion stage; 15 flies of each genotype were required for parallel experiments. The sleep and activity of the experimental flies were monitored by the *Drosophila* Activity Monitor (DAM) system (TriKinetics, USA). The selected flies were raised in standard food vials until they were monitored, then they were moved into 65 mm × 5 mm glass tubes (Wuhan Yihong, China) containing solely 5% sucrose (Sangon Biotech, China) and 2% agar (Sangon Biotech, China). Subsequently, glass tubes with experimental flies were placed in the DAM system which was set in 12-hour LD conditions for the test. LD conditions were light-on at 9 am and light-off at 9 pm. Data collection started after the flies were acclimated to the environment for 3 to 5 days(Song et al., 2017). Data records of experimental activities were binned in one-minute periods in LD for three days. Flies were regarded to be sleeping when they were inactive for at least 5 minutes. Flies were implied to have died when their whole period of activity was less than 10 minutes, and the data were excluded. Flies' sleep duration and parameters related to sleep behavior were analyzed by R software. Conventional sleep plots were portrayed by calculating the average amount of sleep duration within 30 minutes of experimental flies.

RNA extraction and sequencing

The flies were placed in 1 mL TRIzol (Invitrogen, USA), and we used forceps to rapidly break down the brains of the adult flies rapidly. Almost 20 heads of each genotype were saved in a 1.5 mL microcentrifuge tube with 200 μL of TRIzol. There were 3-4 replicates for each genotype. RNA extraction and purification were performed using TRIzol. The RNA was eluted with nuclease-free water, then a NanoDrop 2000 (Thermo Scientific, USA) was used to evaluate of RNA purity and concentration.

RNA-sequencing was performed on 3-4 replicates of RNA samples from each of *elav-GAL4*, *elav>Ten-m-RNAi*, and *elav>Ten-m* groups. The sample libraries were prepared according to the standard process of the TruSeq RNA Sample Prep Kit v2 (Illumina, USA). The final libraries were determined by Qubit 2100 (Thermo Scientific, USA) and Bioanalyzer (Illumina, USA) and paired-end sequencing was performed on an Illumina HiSeq X-Ten System (Illumina, USA), with a read length of 2 × 150 bp.

Adapters and low-quality reads were removed from the raw data using Trimmomatic (v0.36) (Bolger et al., 2014). TopHat (v2.1.1) was used to align the RNA-seq reads to a reference genome (BDGP5.25) with the short-read aligner Bowtie2 (v2.3.4) (Kim et al., 2013) (Langmead and Salzberg, 2012). Cufflinks (v2.2.1) was used to analyze the BAM files, including assembling the transcripts from the aligned reads and estimating their abundances using a Fragments Per Kilobase of transcript per Million mapped reads (FPKM)-based algorithm (Trapnell et al., 2012). HTSeq (v0.10) was used to generate the read count files for each gene (Anders et al., 2015). Then, DESeq2 (v1.36.0) was used to identify DEGs, which were selected with log2 (fold change) >1 or log2 (fold change) <-1 and with statistical significance (adjusted p-value <0.05) (Love et al., 2014). GO and KEGG pathway enrichment analysis of DEGs was performed using the Database for Annotation, Visualization and Integrated Discovery (DAVID) functional annotation tool (v6.8).

QUANTIFICATION AND STATISTICAL ANALYSIS

In courtship conditioning assay, the courtship index (CI) was calculated as the percentage of male courtship duration within 10 minutes. The learning index (LI) was calculated using the mean CIs, LI = [CI naive – CI trained]/CI naive (Keleman et al., 2012). As the distributions of LIs are different between groups, LIs were used for the permutation test with 100,000 random permutations to compare between groups, and the data were processed with R software. One-tail testing against the null hypothesis was used in the comparison. The Mann–Whitney U test was used for CIs.

In aggression assay and sleep assay, all behavior data analyses were performed using Sigma Plot (v14.0) and SPSS (v22.0). For multiple comparisons, one-way ANOVA followed by post hoc Tukey were used, except for the comparison of nonparametrically distributed data where the Kruskal–Wallis test was used.